Liquid Ordered and Gel Phases of Lipid Bilayers: Fluorescent Probes Reveal Close Fluidity but Different Hydration

Gora M'Baye, Yves Mély, Guy Duportail, and Andrey S. Klymchenko
Photophysique des Interactions Biomoléculaires, UMR 7175 du CNRS, Institut Gilbert Laustriat, Faculté de Pharmacie, Université Louis Pasteur, 67401 Illkirch, France

ABSTRACT Hydration and fluidity of lipid bilayers in different phase states were studied using fluorescent probes selectively located at the interface. The probe of hydration was a recently developed 3-hydroxyflavone derivative, which is highly sensitive to the environment, whereas the probe of fluidity was the diphenylhexatriene derivative, 1-[4-(trimethylamino)phenyl]-6-phenylhexa-1,3,5-triene. By variation of the cholesterol content and temperature in large unilamellar vesicles composed of sphingomyelin or dipalmitoylphosphatidylcholine, we generated different phases: gel, liquid ordered (raft), liquid crystalline, and liquid disordered (considered as liquid crystalline phase with cholesterol). For these four phases, the hydration increases in the following order: liquid ordered $\ll$ gel $\approx$ liquid disordered $<$ liquid crystalline. The membrane fluidity shows a somewhat different trend, namely liquid ordered $\approx$ gel $<$ liquid disordered $<$ liquid crystalline. Thus, gel and liquid ordered phases exhibit similar fluidity, whereas the last phase is significantly less hydrated. We expect that cholesterol due to its specific H-bonding interactions with lipids and its ability to fill the voids in lipid bilayers expels efficiently water molecules from the highly ordered gel phase to form the liquid ordered phase. In this study, the liquid ordered (raft) and gel phases are for the first time clearly distinguished by their strong difference in hydration.

INTRODUCTION

Cholesterol is a major constituent of mammalian plasma membranes that can induce domain formation (1). In this respect, microdomains rich in cholesterol and sphingomyelin, known as ''lipid rafts'', have received a huge attention because they are believed to be involved in regulation of cell functions such as signal transduction, lipid trafficking and membrane protein activity (2–5). Raft domains can also form in synthetic lipid vesicles and supported lipid bilayers containing saturated glycerophospholipids or sphingolipids and cholesterol (6–9). Rafts are characterized by a tight packing of the lipid saturated acyl chains (10,11). In biomembranes, rafts likely exist in a liquid-ordered state (L_o), and behave like islands floating in a sea of loosely-packed domains of unsaturated glycerophospholipids being in a liquid disordered (fluid) state (L_d). Comparing mixtures with and without cholesterol shows that cholesterol can promote phase separation (12,13) due to its favorable packing interactions with saturated lipids.

To better understand the mechanisms governing the cholesterol-induced domain formation, more information should be obtained on the molecular interactions between cholesterol and sphingomyelin (SM) or other saturated phospholipids.

In addition to hydrophobic and van der Waals forces (1), the 3-OH group of cholesterol in glycerophospholipids vesicles likely forms H-bonds with sn_2-carbonyl and phosphate groups in the interfacial bilayer region (14–17). Moreover, SM may interact with the 3-OH group of cholesterol by its phosphate oxygen, whereas its NH group is involved in intermolecular H-bonds between SM molecules (18–21). Though H-bonds are important in the interfacial region of SM and dipalmitoylphosphatidylcholine (DPPC) bilayers, their role in the formation of the L_o phase has to be confirmed.

In this respect, hydration of the bilayer interface is an important parameter, because the formation/destruction of H-bonds in this region should control the presence of water molecules. Water associates with the headgroups of phospholipids via H-bonds (22) to form the hydration layer. In addition, water penetrates into lipid bilayers, fitting packing defects between fatty acyl chains (23), thus constituting an interchain hydration. Thus, in glycerophospholipids, sn_1- and especially sn_2-carbonyls are well hydrated. Previous studies using the Laurdan probe suggested that addition of cholesterol to bilayers of saturated (dimyristoylphosphatidylcholine) lipids in gel (L_β) phase decreases their hydration (24). Because cholesterol likely generates a L_o phase, this observed change in hydration is of interest. However, because the location of Laurdan is not clearly defined (25) due to the absence of any anchoring group, this hydration decrease can hardly be assigned to a particular region of the bilayer.

To probe the hydration of the membrane, we developed 3-hydroxyflavone (3HF) fluorescent probes that exhibit an excited-state intramolecular proton transfer (ESIPT) reaction, resulting in a dual emission highly sensitive to the environment (26–29). In addition to solvent polarity, these dyes exhibit a high sensitivity to specific H-bonding interactions with protic solvents (including water) that suppress the ESIPT reaction (29–32). This sensitivity to water was applied to

Submitted December 10, 2007, and accepted for publication March 28, 2008.

Address reprint requests to Dr. Andrey S. Klymchenko, Photophysique des Interactions Biomoléculaires, UMR 7175 du CNRS, Institut Gilbert Laustriat, Faculté de Pharmacie, Université Louis Pasteur, 67401 Illkirch, France. Tel.: 33-390-244255; Fax: 33-390-244313; aklymchenko@pharma.u-strasbg.fr.

Editor: Lukas K. Tamm.

0006-3495/08/08/1217/09 $2.00

doi: 10.1529/biophysj.107.127480

sense hydration at specific regions of the lipid bilayers (25,33). Notably, we synthesized dyes bearing a trialkylammonium anchoring group, which localizes the 3HF fluorophore in the glycerol region of the lipid bilayer (34). These probes are present in the lipid bilayer both in H-bond-free and H-bonded (linked to water) forms (Fig. 1). The relative contribution of the two forms, obtained by a deconvolution of the fluorescence spectra, provides a quantitative description of the bilayer hydration (25,33). In this study, we used the well-characterized probe *N*-[(4′-*N*,*N*-diethylamino)-3-hydroxy-6-flavonyl]methyl-*N*,*N*-dimethyloctyl ammonium bromide (F2N8) (Fig. 1) to study the hydration of SM and DPPC bilayers, which form in the presence of cholesterol pure L_o phase. In parallel, we used an anchored DPH derivative (1-[4-(trimethylamino)phenyl]-6-phenylhexa-1,3,5-triene [TMA-DPH]) to correlate the changes in hydration with the changes in the fluidity at the similar depth within the bilayer (Fig. 1). Surprisingly, a comparison between the L_β and L_o phases did not show any correlation between these two parameters. Indeed, although TMA-DPH shows nearly no difference of fluidity between these two phases, F2N8 shows a dramatic decrease of the hydration of the L_o phase as compared to the L_β phase. This clear difference between L_β and L_o phases provides new insights for further understanding the role of the L_o phase in biological membranes.

MATERIALS AND METHODS

DPPC, dioleoylphosphatidylcholine (DOPC), and cholesterol were purchased from Sigma-Aldrich (Lyon, France). Bovine brain sphingomyelin was from Avanti Polar Lipids (Alabaster, AL). TMA-DPH was from Molecular Probes (Leiden, Netherlands). Probe F2N8 was synthesized as described (34). This probe was pure according to thin layer chromatography, ^{1}H-NMR data, absorption, and fluorescence spectra in organic solvents.

Large unilamellar vesicles (LUV) were obtained by the classical extrusion method as described previously (36). Briefly, a suspension of multilamellar vesicles was extruded by using a Lipex Biomembranes extruder (Vancouver, Canada). The size of the filters was first 0.2 μm (7 passages) and thereafter 0.1 μm (10 passages). This generates monodisperse LUVs with a mean diameter of 0.11 μm as measured with a Malvern Zetamaster 300 (Malvern, UK). LUVs were labeled by adding aliquots (generally 2 μl) of probe stock solutions (2 mM, in dimethyl sulfoxide for F2N8 and in dimethylformamide for TMA-DPH) to 2-ml solutions of vesicles. Because the binding kinetics is very rapid for both probes, the fluorescence experiments were processed a few minutes after addition of the aliquot. A 15-mM phosphate-citrate, pH 7.0 buffer was used in all experiments (37). Concentrations of the probes and lipids were 2 and 200 μM, respectively.

Fluorescence spectra were recorded on a Horiba Jobin-Yvon Fluoromax 3 (Longjumeau, France) spectrofluorometer and corrected by subtracting the spectra of the corresponding blank vesicles. The excitation wavelength of F2N8 was 400 nm. Fluorescence anisotropies of TMA-DPH labeled vesicles were measured on a SLM 8000 spectrofluorimeter in the T-format configuration. The excitation wavelength was 360 nm and the emitted light was monitored at 435 nm with an appropriate interference filter from Schott (Mainz, Germany). A home-built device ensured the automatic rotation of the excitation polarizer, allowing continuous measurement of the anisotropy. To obtain the thermotropic profiles, the temperature was regulated with a programmed Huber CC2 water bath (Offenburg, Germany). The heating rate was fixed at 1.5°C/min and the temperature was continuously monitored with a thermocouple inserted into the cuvette. Pairs of data (r and T, °C) were processed with the Biokine software from Biologic (Claix, France). For each fluorescence anisotropy value, the estimated absolute error is $\Delta r \leq 0.002$.

Deconvolution of probe F2N8 fluorescence into three bands (N*, H-N* and T*) was carried out by using the Siano software kindly provided by Dr. A.O. Doroshenko (Kharkov, Ukraine). The program is based on an iterative nonlinear least-squares method that is itself based on the Fletcher-Powell algorithm. The individual emission bands were approximated by a log-normal function (38) that accounts for several parameters (maximal amplitude, I_{max}, spectral maximum position, ν_{max}, and position of half-maximum amplitudes, ν_1 and ν_2, for the blue and red parts of the band, respectively). The program Siano operates with the shape parameters of the log-normal function are directly connected with the full width at the half-maximum, FWHM = $\nu_1 - \nu_2$, and band asymmetry, $P = (\nu_1 - \nu_{max})/(\nu_{max} - \nu_2)$, and allows approximating the asymmetric bands in absorption and fluorescence spectra. To obtain more stable results of deconvolution, several parameters were fixed based on previous data in organic solvents and LUVs (25,29,33). Thus, the FWHM of the two short-wavelength bands (N* and H-N*) were fixed at 3000 cm^{-1}, except for SM-containing vesicles, where FWHM of the N* band was fixed at 2600 cm^{-1}. The last value was directly determined from the F2N8 emission spectrum for SM vesicles containing 35% cholesterol, where contribution of the H-N* band is almost negligible. For the H-N* band, the asymmetry was fixed at 0.9, whereas the band position was fixed at 18,400 cm^{-1} and 19,200 cm^{-1} for vesicles containing DPPC and SM, respectively. The other parameters, i.e., asymmetry of N* and T* bands, width

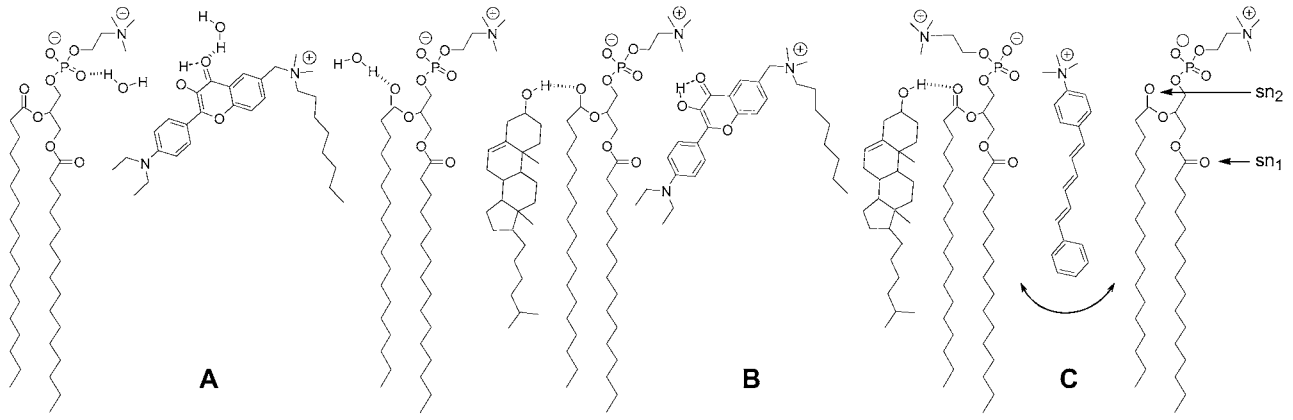

FIGURE 1 Schematic representation of a lipid bilayer leaflet, and location of the F2N8 (*A* and *B*) and TMA-DPH (*C*) probes, water molecules and cholesterol. Two ground-state forms of F2N8 are shown: H-bonded (*A*) and H-bond free (*B*). The arrows in (*C*) imply the wobbling motion of TMA-DPH in the bilayer. The location of the phospholipid functional groups is based on x-rays and neutron diffraction studies (35).

of the T* band and relative intensities of the bands, were allowed to vary. Examples of deconvolution are presented in Fig. 2, *B* and *C*. The resulting fluorescence intensities of the separated N*, H-N* and T* bands (I_{N*}, $I_{H\text{-}N*}$, and I_{T*}) were used for calculation of the hydration parameter, which was expressed as the ratio of the emission intensity of the hydrated (H-N*) form to the summed intensities of the nonhydrated (N* and T*) forms. Taking into account that the FWHM for the T* band is ~2.5-fold narrower than for the N* and H-N* bands, the hydration can be estimated as $I_{H\text{-}N*}/(I_{N*} + 0.4 \times I_{T*})$ (25,33).

RESULTS

Fluorescence spectra of F2N8 in LUV and preference of the probe for the fluid phase

The fluorescence spectra of probe F2N8 incorporated in three types of LUVs of different composition were recorded at 20°C (Fig. 2). The first type corresponds to DOPC or SM LUVs. The second type of LUVs were obtained by adding 35 mol % cholesterol to the previous ones to obtain either pure nonraft vesicles (DOPC/Chol) in a L_d phase, or pure raft vesicles (SM/Chol) in a L_o phase. Finally, LUVs were prepared with a ternary mixture (DOPC/SM/Chol) in the molar ratio 1:1:0.7. In all cases, F2N8 exhibits a dual emission spectrum. According to the previous studies in other lipid vesicles, this apparent dual emission is composed of three overlapping bands: the emission of the normal (N*) and tautomer (T*) forms, resulting from the ESIPT reaction, and the emission of the H-bonded (hydrated) form (H-N*) that does not participate to ESIPT. The emission band resulting from the H-N* form, which is located between the N* and T* emission bands, can be obtained by deconvoluting the emission spectrum (25,33). The relative contribution of this H-N* species is mainly responsible of the differences between the spectra in Fig. 2.

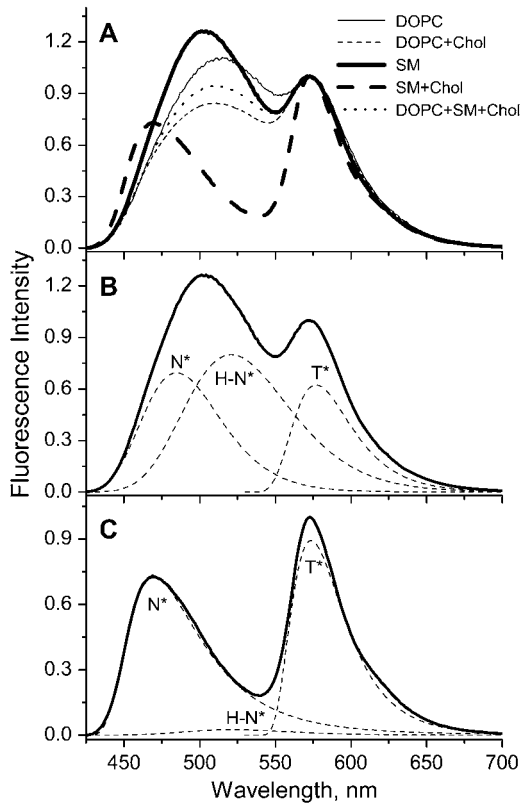

FIGURE 2 Fluorescence emission spectra of probe F2N8 in LUVs of different lipid composition. (*A*) When present, cholesterol (Chol) was added at 35 mol % with respect to phospholipids. In the ternary mixture, the molar ratio of lipids was DOPC/SM/Chol = 1/1/0.7. The spectra were normalized at the T* band maximum. Excitation wavelength was 400 nm. (*B* and *C*) Results of the three-band deconvolution of the fluorescence spectra of F2N8 in LUV composed either of SM (*B*) or SM/Chol (*C*).

In both single component vesicles, F2N8 emission shows a rather high relative intensity of the short-wavelength band. Noticeably, this band is blue-shifted in SM vesicles with respect to that in DOPC vesicles. Addition of 35 mol % of cholesterol decreases the relative intensity of the short-wavelength band for both DOPC and SM vesicles, but the effect appears much higher with SM vesicles, as shown by the important depression in the middle of the spectrum. Moreover, in SM vesicles, the short-wavelength band shifts dramatically to the blue. These effects could be connected to a decrease of polarity and hydration in the probe environment (25,33). The much stronger effects in SM vesicles can be tentatively related to their phase transition from the gel phase to the liquid ordered (raft) phase on addition of cholesterol, whereas DOPC vesicles preserve a liquid disordered phase.

The partitioning preference of F2N8 between liquid ordered or liquid disordered phases can be evaluated with the ternary mixture DOPC/SM/Chol, which contains coexisting raft and nonraft domains (6–9). The fluorescence spectrum of the probe in the ternary mixture (Fig. 2) resembles the spectrum in DOPC/Chol vesicles containing only nonraft domains, suggesting that F2N8 preferentially partitions into nonraft (L_d) domains.

Cholesterol-induced formation of liquid ordered phase

Because F2N8 shows a poor preference for the raft phase, all-raft systems, namely mixtures of SM or DPPC with cholesterol, but without DOPC were used to study the behavior of the probe in rafts. We prepared and labeled several batches of LUVs composed of SM or DPPC with varying amounts of cholesterol from 0 to 35 mol %. As shown in Fig. 3 *A*, addition of cholesterol to SM vesicles in their gel phase (20°C) gradually modifies the fluorescence emission spectra. The short-wavelength band decreases and shifts to the blue when the cholesterol ratio increases, especially at the higher ratios. As a consequence, we observe a strong separation of the two emission maxima, together with a concomitant depression of the middle of the spectra, around 540 nm. Meantime, when the emission spectra are recorded at 60°C, the effect of cholesterol appears much weaker (Fig. 3 *B*). Both the de-

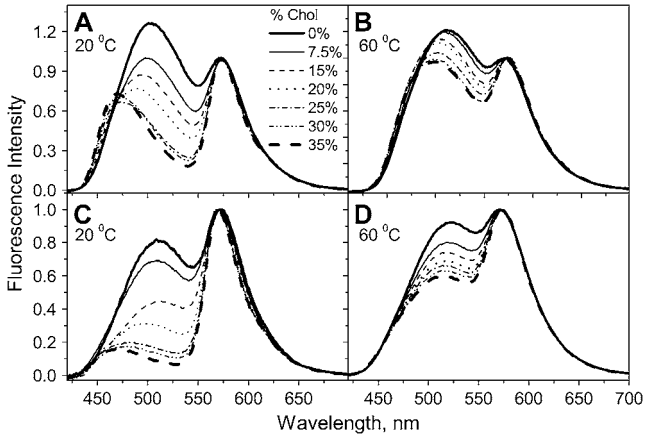

FIGURE 3 Fluorescence spectra of F2N8 probe in SM (*A* and *B*) and DPPC (*C* and *D*) vesicles at different mol % of cholesterol, at 20°C (*A* and *C*) and 60°C (*B* and *D*).

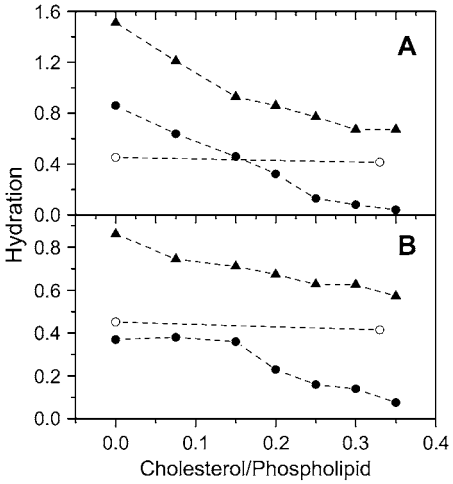

FIGURE 4 Hydration as a function of cholesterol/phospholipid ratio in SM (*A*) and DPPC (*B*) vesicles at 20°C (*solid circles*) and 60°C (*triangles*). Corresponding data for EYPC (*open circles*) at 20°C are presented for comparison.

crease of the relative intensity of the short-wavelength band and its blue shift are small, and consequently, the separation between the two bands is much less pronounced than at 20°C.

To further characterize the spectroscopic response of the probe on addition of cholesterol to SM vesicles, we deconvoluted the fluorescence spectra into three bands (N*, H-N* and T*) as described in Materials and Methods. The results of the deconvolution of SM and SM/Chol vesicles are presented in Fig. 2, *B* and *C*, respectively. In pure SM vesicles, the N*, H-N*, and T* bands contribute to similar extents, whereas in the presence of 35% of cholesterol (SM/Chol), the contribution of the H-N* band is almost negligible compared to that of the N* and T* bands. This shows that at 20°C, addition of 35% of cholesterol decreases the hydration of the SM bilayers more than 20-fold (Fig. 4 *A*). In contrast, at 60°C, this dehydration is much lower with only a 2.3-fold decrease (Fig. 4 *B*). Interestingly, in EYPC (33) and DOPC vesicles (Fig. 2), which are in a fluid phase at room temperature, the dehydration effect of cholesterol is also quite weak. Thus, strong dehydration is observed only on addition of cholesterol to the SM bilayers in the gel phase. This is important because at 20°C, high concentrations of cholesterol in SM vesicles lead to the formation of raft domains, whereas at 60°C in SM vesicles, as well as in EYPC and DOPC vesicles at 20°C, raft domains are not expected. Thus, we conclude that raft formation results in a strong dehydration of the membrane, at least at the depth sensed by the probe.

Mixtures of cholesterol and saturated DPPC are also known to induce raft phases in model systems. Therefore, we carried out the same experiments with DPPC vesicles as with SM vesicles. A similar evolution of F2N8 emission spectra is observed, with a progressive decrease in the relative intensity of the short-wavelength band together with its blue shift for increasing concentrations of cholesterol at 20°C (Fig. 3 *C*). Moreover, at 60°C, we also observe limited changes in the dual emission, with almost no blue-shift of the short-wavelength band (Fig. 3 *D*). In DPPC vesicles, a decreasing hydration at 20°C was also observed with increasing amounts of cholesterol (Fig. 4 *B*). Again, this decrease is much larger than that observed at 60°C. Thus, DPPC and SM vesicles show the same strong membrane dehydration with increasing cholesterol ratio, which is likely connected with the formation of rafts within the membrane. According to the phase diagram of SM/Chol mixtures (39), phase separation between raft and gel phases is observed above 10 mol % of cholesterol. Therefore, the progressive dehydration on addition of cholesterol is probably connected with the increase in the raft-to-gel phase ratio within the bilayers.

To get further information on the effect of the addition of cholesterol to SM and DPPC vesicles, we carried out fluorescence anisotropy experiments with the TMA-DPH probe to measure the bilayer fluidity. As F2N8, TMA-DPH is anchored at the bilayer interface by a trialkylammonium group (Fig. 1 *C*), thus sensing only the upper part of the bilayer (40). This means that we can put in balance the respective information (hydration and fluidity) given by this pair of probes. As shown in Fig. 5, cholesterol does not modify significantly the TMA-DPH fluorescence anisotropy of both SM and DPPC bilayers at 20°C. In contrast, we observe a significant increase in the fluorescence anisotropy with increasing cholesterol at 60°C, where no raft phase is expected. Both observations confirm that in the fluid phase, addition of cholesterol decreases the fluidity of the bilayer, whereas in the gel phase, cholesterol has only a limited influence (41,42). Thus, the gel (L_β) and liquid ordered (L_o) phases show strong differences in their hydration, but only limited differences in their fluidity.

Temperature-driven transitions

Temperature is another important parameter controlling raft formation. Therefore, we studied the temperature-dependent

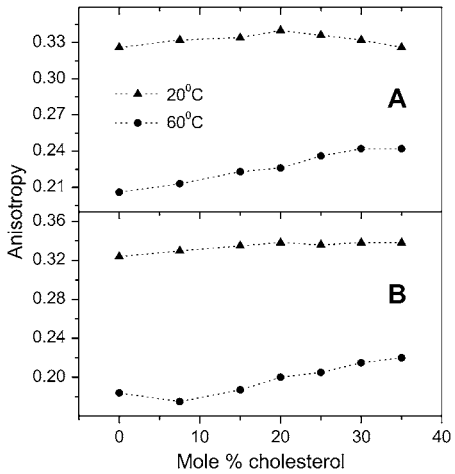

FIGURE 5 Fluorescence anisotropy of TMA-DPH as a function of the cholesterol ratio in SM (*A*) and DPPC (*B*) vesicles. The experimental error: $\Delta r \leq 0.002$.

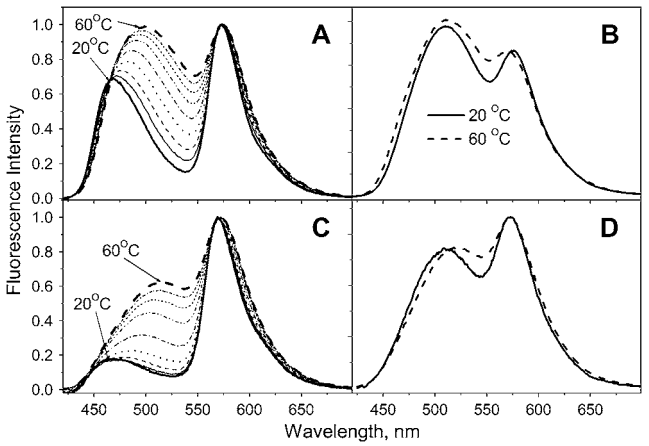

FIGURE 6 Temperature effect on the fluorescence spectra of F2N8 in LUVs composed of SM/cholesterol (*A*), SM (*B*), DPPC/cholesterol (*C*), and DPPC (*D*). Fluorescence spectra were normalized at the T* maximum. In (*A*) and (*C*), the spectra were recorded by changing the temperature by 5°C steps. Excitation wavelength was 400 nm.

transitions of raft systems ($L_o \rightarrow L_d$) and compared them with the classical gel-liquid crystalline ($L_\beta \rightarrow L_\alpha$) transition in single-component vesicles. It should be noted that we use the term L_α for the liquid-crystalline phase in pure phospholipid vesicles, whereas L_d is defined as a L_α phase containing cholesterol.

We first considered the temperature-dependence of F2N8 emission spectra in either pure L_β phase vesicles (SM or DPPC) or pure L_o phase vesicles (SM or DPPC with 35% cholesterol), to infer the dependence of their hydration on temperature. In lipid bilayers composed of DPPC/Chol and SM/Chol mixtures, the increase in temperature, which results in $L_o \rightarrow L_d$ phase transition, modifies strongly the dual emission spectra of the probe (Fig. 6, *A* and *C*). Increasing the temperature from 15 to 60°C strongly increases the hydration of SM/Chol and DPPC/Chol bilayers, by 46-fold and 10-fold, respectively (Fig. 7). The hydration increases gradually over all the studied temperature range, indicating no particular temperature transition points. According to the phase diagrams for these lipid mixtures, the $L_o \rightarrow L_d$ transition should occur at temperatures around or higher to the temperature (≈40°C) of the $L_\beta \rightarrow L_\alpha$ phase transition of the corresponding pure phospholipids (15,39). However, changes in the lipid hydration occur already at 20°C, indicating that the L_d phase can form at lower temperatures than expected, probably because the $L_o \rightarrow L_d$ transition is much broader than the $L_\beta \rightarrow L_\alpha$ phase transition. To further investigate the temperature effects, we studied the $L_\beta \rightarrow L_\alpha$ phase transition in pure SM and DPPC vesicles by using F2N8. Surprisingly, on the phase transition, we observe only limited changes in the emission spectra (Fig. 6, *B* and *D*). According to the deconvolution analysis, the hydration in pure SM and DPPC vesicles increases 1.3- and 2-fold, respectively, on changing temperature from 15 to 60°C (Fig. 7), which is much smaller than the hydration increase during the $L_o \rightarrow L_d$ transition.

The probe F2N8 is nonfluorescent in bulk water. Moreover, according to our previous titration experiments in DOPC vesicles (34) at high probe/lipid ratios (>1/100), it shows a linear dependence of its intensity on the lipid concentration proving that it does not exhibit any significant self-quenching in lipid vesicles. Therefore, the fluorescence intensity of F2N8 can be used to characterize the number of the probe binding sites within the lipid bilayer. As shown in Fig. 8, in pure SM and DPPC vesicles, an increase in the fluorescence intensity is observed around the transition temperature, whereas above this temperature the fluorescence intensity slightly decreases. As expected, the transition from the highly ordered L_β phase to the liquid-crystalline L_α phase increases the number of bilayer defects and thus favors the incorporation of small dye molecules. Above the transition temperature, the effects of thermal quenching prevail and

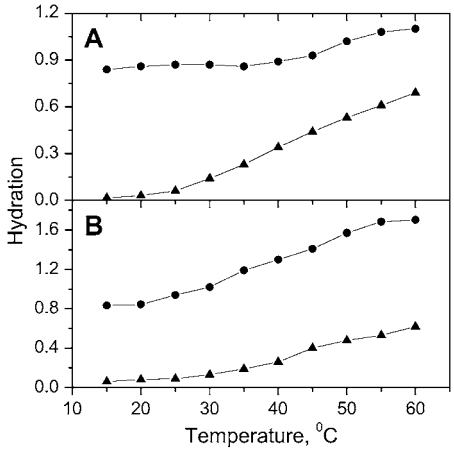

FIGURE 7 Temperature dependence of the hydration in LUVs, as measured by probe F2N8. LUVS were composed of SM (*A*) and DPPC (*B*) without (*circles*) and with 35 mol % of cholesterol (*triangles*).

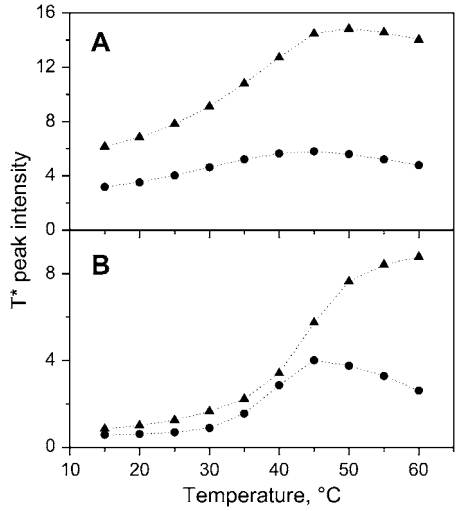

FIGURE 8 Temperature dependence of F2N8 fluorescence intensity at the T* maximum wavelength (575 nm) in LUVs. The LUVs were composed of SM (*A*) and DPPC (*B*) without (*circles*) and with 35 mol % of cholesterol (*triangles*).

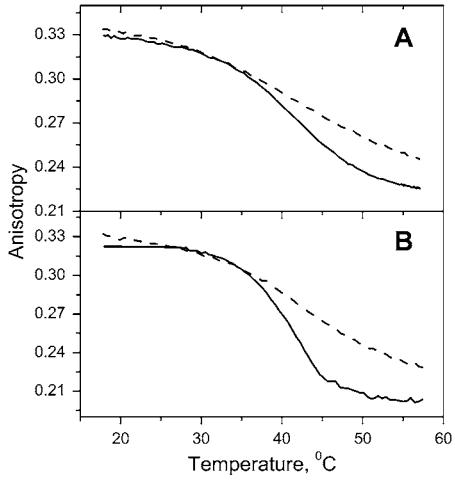

FIGURE 9 Thermotropic fluorescence anisotropy of TMA-DPH in LUVs composed of SM (*A*) and DPPC (*B*) without (*solid line*) and with 35 mol % of cholesterol (*dashed line*). The experimental error: $\Delta r \leq 0.002$.

thus decrease the fluorescence intensity. For vesicles containing cholesterol, we observe an even stronger increase in the fluorescence intensity of F2N8 around the transition temperature. Similarly to the thermotropic $L_\beta \rightarrow L_\alpha$ transition, the transition $L_o \rightarrow L_d$ increases the number of binding sites for the probe. This increase in the fluorescence intensity with temperature is in line with the observed increase in hydration, because the bilayer interior should become more accessible not only to the probes, but also to bulk water molecules.

We also characterized the temperature-dependent transitions by monitoring the thermotropic fluorescence anisotropy profiles for the different phospholipid vesicles labeled with TMA-DPH (Fig. 9). In single component vesicles, the $L_\beta \rightarrow L_\alpha$ phase transition is characterized by a cooperative decrease of the anisotropy centered at the so-called transition temperature. In contrast, for vesicles containing 35% cholesterol, the differences between the two limiting phases (L_o and L_d) is less pronounced and the phase transition is broader. These results are fully in line with the literature (41,42).

Thus, the changes in the membrane fluidity do not correlate with the hydration changes. Indeed, although the $L_o \rightarrow L_d$ transition modifies the bilayer fluidity to a lesser extent than the $L_\beta \rightarrow L_\alpha$ transition does, the opposite is observed for the bilayer hydration.

Probing the heterogeneity of DPPC/cholesterol lipid bilayers

The dramatic differences in the hydration properties of the L_β and L_o phases prompted us to study lipid vesicles composed of DPPC/Chol mixtures for which, according to their phase diagram, both phases should be simultaneously present (15). Assuming that the affinities of F2N8 for the L_β and L_o phases are different, one should observe an evolution of its fluorescence spectrum when increasing the probe concentration with respect to the lipid concentration.

With pure DPPC vesicles, we observe a steep increase in the fluorescence intensity with a plateau at a probe concentration above 2 μM (Fig. 10 *A*). This plateau indicates that the binding sites of the bilayer are saturated and that, as previously mentioned, no probe self-quenching is observed at the studied probe concentrations. Furthermore, the increase in the probe concentration does not significantly change the ratio of its two emission bands, suggesting the existence of only one type of binding sites in the L_β phase of DPPC vesicles. In vesicles containing 15 mol % of cholesterol, the increase in the probe concentration results in a less steep increase of its fluorescence intensity, with a fluorescence plateau only at concentrations above 4 μM. Moreover, in this case, the emission spectrum depends strongly on the probe concentration, with a gradual decrease of the short-wavelength band relative intensity (Fig. 10 *B*). Remarkably, at low probe concentrations, the emission spectrum in 15 mol % Chol-containing vesicles resembles that in pure DPPC vesicles. In contrast, with increasing probe concentration, the spectrum gradually changes into a spectrum that corresponds to an average between the spectra in pure DPPC vesicles and 35 mol % Chol-containing vesicles (Fig. 10 *B*). These observations indicate that at low concentrations, F2N8 binds preferentially the L_β phase, whereas at higher concentrations, the binding sites of the gel phase are saturated and the probe binds also the L_o phase. Therefore, at high probe concentrations, both phases are labeled so that the final emission spectrum corresponds to the superposition of the spectra in the two phases. Thus, our hydration sensitive probe allows monitoring the simultaneous presence of the two separated L_o and L_β phases in vesicles composed of DPPC and 15 mol % Chol.

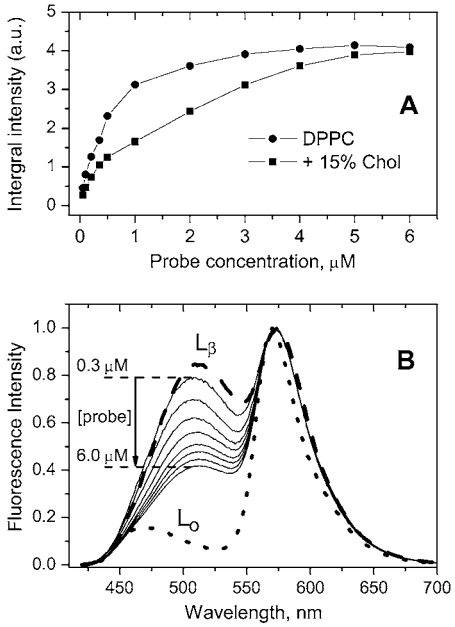

FIGURE 10 Dependence of the fluorescence properties of F2N8 on its concentration in LUVs composed either of DPPC or DPPC with 15 mol % of cholesterol. Lipid concentration was 0.2 mM. (*A*) Fluorescence intensity versus probe concentration and (*B*) fluorescence spectra of probe in different conditions: 0.2 μM probe in LUV composed of DPPC (*dashed line*, L_β) or DPPC and 35 mol % of cholesterol (*dotted line*, L_o). Solid lines correspond to spectra in LUV composed of DPPC and 15 mol % of cholesterol at different probe concentrations: 0.3, 0.5, 1.0, 2.0, 3.0, 4.0, 5.0, 6.0 μM.

DISCUSSION

Phase separation between lipids in different physical states is not exclusive to the problem of raft formation since this phenomenon has been well characterized in model membranes, most often between liquid-crystalline phase (L_α) and solid-like gel phase (L_β). Although the L_d phase can be considered as a liquid-crystalline (L_α) phase, the positioning of the L_o state is less evident. Indeed, the L_β gel phase is the most familiar state in which acyl chains are highly ordered (43,44). However, though the acyl chains are also extended and tightly packed in the L_o phase, this state differs from the L_β phase by the higher lateral mobility of the lipids (4), probably due to the high concentration of cholesterol.

In this study, the phospholipid membranes were described mainly in terms of hydration and fluidity, these two parameters being followed independently by two different probes. The fluidity of the membrane was described from the fluorescence anisotropy of TMA-DPH, whereas the hydration was estimated from the relative contribution of the hydrated form of F2N8 to its emission spectrum. According to previous studies, the locations of TMA-DPH and F2N8 in the bilayer are relatively close, namely 9 Å (45) and 13–16 Å (33,34), respectively, from the bilayer center (Fig. 1). Therefore, both fluidity and hydration parameters are determined around the glycerol level (or its equivalence for SM) of the membrane interface.

Our fluidity data are in line with previous data using DPH and its derivatives (41,42). Indeed, the temperature-driven phase transitions of DPPC vesicles containing either no or 35 mol % of cholesterol (Fig. 11 *A*) indicate that the fluidities (inversely related to the anisotropies) of the L_β and L_o phases are similar and much lower than the fluidities of the L_d and L_α phases. In contrast, the bilayer hydration shows a very different phase-dependent behavior. For both SM and DPPC pure vesicles, the bilayer hydration is the highest in L_α and remains relatively high for the L_β and L_d phases, whereas the L_o phase (at 20°C) is characterized by a very low hydration (Fig. 11 *A*). Thus, comparison of L_β and L_o phases show that the fluidity and hydration do not correlate because the fluidity is similar in these two phases although their hydration is strongly different. In the L_α phase, the fluidity correlates well with the hydration because the increase in the fluidity as a result of temperature increase or lower cholesterol content is accompanied by an increase in the hydration. This is not surprising, because when the lipid dynamics increases, the membrane becomes more accessible to water molecules due to temporary defects and voids in the lipid bilayer.

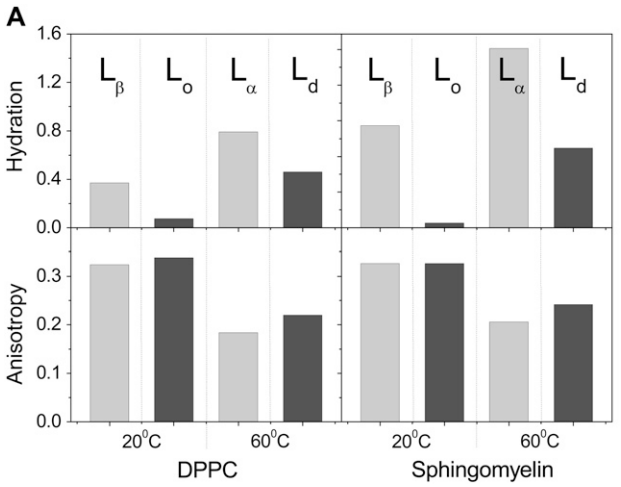

FIGURE 11 Effect of cholesterol on raft-containing bilayers (*A*) Comparison of the hydration and fluidity evaluated by F2N8 and TMA-DPH in LUVs composed of raft-forming phospholipids. Light gray bars correspond to pure phospholipids (DPPC or SM). Dark gray bars correspond to vesicles containing 35 mol % of cholesterol. (*B*) Schematic model of the effect of cholesterol (*long gray bars*) on the presence of the water molecules (*small gray ellipsoids*) near the phospholipid headgroups.

Then, the question arises on how the addition of cholesterol to a L_β phase, to induce a L_o phase, may decrease the hydration? We expect that this phenomenon is based mainly on specific interactions of cholesterol with the raft forming lipids, SM, or saturated glycerophospholipids. It is well established that cholesterol forms specific H-bonds with lipids due to its 3-OH group. Moreover, it has been shown that cholesterol forms H-bonds with the sn_2-carbonyl (14,15) and/or with the phosphate oxygens of the polar heads of DDPC phospholipids (18–21). These H-bonds could substitute the H-bonds occurring with water molecules, resulting in an expulsion of water from the bilayer. This is in line with a previous report (24) with the Laurdan probe showing that addition of cholesterol to dimyristoylphosphatidylcholine vesicles in their gel phase results in their dehydration. However, Laurdan does not allow localizing precisely the region of the bilayer that undergoes dehydration. In contrast, the hydration-sensitive probe F2N8 is more precisely located and thus can selectively detect the hydration differences between the L_o and L_β phases. Indeed, according to our previous parallax quenching measurements (33,34), the H-bonded and H-bond free forms of F2N8 locate at 16 and 13 Å, respectively, from the bilayer center so that the hydration is estimated within this rather narrow range of depths corresponding to the location of the sn_2-carbonyl and phosphate groups of the bilayer (Fig. 1). However, the average location of the probe in a L_o phase is thought to be deeper (close to 13 Å) than in other phases including the L_β phase, because cholesterol favors H-bond free form of the probe.

The fluidity of the L_β phase does not change significantly on its transition to the L_o phase (on addition of cholesterol), probably because the lipid order in the former is already high and cannot be further increased by cholesterol. In contrast, the order of the hydrophobic fatty acid chains is strongly modified during the thermotropic $L_\beta \rightarrow L_\alpha$ transition with probably a less pronounced effect of the H-bonding network at the interface level. Thus, although the L_o and L_β phases are both characterized by a high order of their hydrophobic hydrocarbon chains, the L_o phase presents, at the membrane interface, a dense H-bonding network of lipids with cholesterol that diminishes its hydration.

In addition to specific H-bonding effects, a nonspecific effect related to changes in the free volume within the lipid bilayer should be considered. Indeed, cholesterol condenses lipid bilayers, which results in a decrease in the surface area per lipid as well as an increase in the bilayer thickness (44,46,47). Moreover, the phosphocholine head-groups in saturated lipids like DPPC and SM are strongly hydrated, thus, occupying a slightly larger area than the two alkyl chains, so that even in the L_β phase some void spaces under the head-groups are available, which might be filled with water molecules (48). These void spaces might also be filled by cholesterol (49) that can expel water molecules from the bilayer (Fig. 11 *B*), without any strong influence on the lipid order.

This observed dehydration at the membrane interface is probably an important characteristic of the so-called raft domains, and could be the main difference between the liquid ordered (L_o) phase and gel phase (L_β). This study is the first demonstration that these two phases, very similar in their fluidity, can be clearly distinguished by their hydration at the level of the carbonyl and phosphate groups of the bilayer. This high dehydration, which can be assigned to specific complexes between raft forming lipids and cholesterol, has probably a strong biological relevance that remains to be elucidated.

E. London is acknowledged for fruitful discussions. G.M. is a fellow from Agence Universitaire de la Francophonie.

This work was supported by the Centre National de la Recherche Scientifique, the Agence Nationale de la Recherche, the Fondation pour la Recherche Médicale, Connectus, and the Université Louis Pasteur.

REFERENCES

1. Ohvo-Rekila, H., B. Ramstedt, P. Leppimaki, and J. P. Slotte. 2002. Cholesterol interactions with phospholipids in membranes. *Prog. Lipid Res.* 41:66–97.
2. Field, K. A., D. Holowka, and B. Baird. 1997. Compartmentalized activation of the high affinity immunoglobulin E receptor within membrane domains. *J. Biol. Chem.* 272:4276–4280.
3. Brown, D. A., and E. London. 1998. Functions of lipid rafts in biological membranes. *Annu. Rev. Cell Dev. Biol.* 14:111–136.
4. Brown, D. A., and E. London. 1998. Structure and origin of ordered lipid domains in biological membranes. *J. Membr. Biol.* 164:103–114.
5. Simons, K., and E. Ikonen. 2000. How cells handle cholesterol. *Science.* 290:1721–1726.
6. Dietrich, C., L. A. Bagatolli, Z. N. Volovyk, N. L. Thompson, M. Levi, K. Jacobson, and E. Gratton. 2001. Lipid rafts reconstituted in model membranes. *Biophys. J.* 80:1417–1428.
7. Veatch, S. L., and S. L. Keller. 2002. Organization in lipid membranes containing cholesterol. *Phys. Rev. Lett.* 89:268101.
8. Veatch, S. L., and S. L. Keller. 2003. Separation of liquid phases in giant vesicles of ternary mixtures of phospholipids and cholesterol. *Biophys. J.* 85:3074–3083.
9. Baumgart, T., S. T. Hess, and W. W. Webb. 2003. Imaging coexisting fluid domains in biomembrane models coupling curvature and line tension. *Nature.* 425:821–824.
10. Ahmed, S. N., D. A. Brown, and E. London. 1997. On the origin of sphingolipid/cholesterol-rich detergent-insoluble cell membranes: physiological concentrations of cholesterol and sphingolipid induce formation of a detergent-insoluble, liquid-ordered lipid phase in model membranes. *Biochemistry.* 36:10944–10953.
11. Schroeder, R. J., S. N. Ahmed, Y. Zhu, E. London, and D. A. Brown. 1998. Cholesterol and sphingolipid enhance the Triton X-100 insolubility of glycosylphosphatidylinositol-anchored proteins by promoting the formation of detergent-insoluble ordered membrane domains. *J. Biol. Chem.* 273:1150–1157.
12. Silvius, J. R., D. del Giudice, and M. Lafleur. 1996. Cholesterol at different bilayer concentrations can promote or antagonize lateral segregation of phospholipids of differing acyl chain length. *Biochemistry.* 35:15198–15208.
13. Polozov, I. V., and K. Gawrisch. 2006. Characterization of the liquid-ordered state by proton MAS NMR. *Biophys. J.* 90:2051–2061.
14. Verma, S. P., and D. F. H. Wallach. 1973. Effects of cholesterol on the infrared dichroism of phosphatide multibilayers. *Biochim. Biophys. Acta.* 330:122–131.

15. Sankaram, M. B., and T. E. Thompson. 1991. Cholesterol-induced fluid-phase immiscibility in membranes. *Proc. Natl. Acad. Sci. USA.* 88:8686–8690.

16. Bittman, R., C. R. Kasireddy, P. Mattjus, and J. P. Slotte. 1994. Interaction of cholesterol with sphingomyelin in monolayers and vesicles. *Biochemistry.* 33:11776–11781.

17. Bhattacharya, S., and S. Haldar. 2000. Interactions between cholesterol and lipids in bilayer membranes. Role of lipid headgroup and hydrocarbon chain-backbone linkage. *Biochim. Biophys. Acta.* 1467:39–53.

18. Talbott, C. M., I. Vorobyov, D. Borchman, K. G. Taylor, D. B. DuPre, and M. C. Yappert. 2000. Conformational studies of sphingolipids by NMR spectroscopy. II. Sphingomyelin. *Biochim. Biophys. Acta.* 1467: 326–337.

19. Mombelli, E., R. Morris, W. Taylor, and F. Fraternali. 2003. Hydrogen bonding propensities of sphingomyelin in solution and in a bilayer assembly: a molecular dynamics study. *Biophys. J.* 84:1507–1517.

20. Niemela, P., M. T. Hyvonen, and I. Vattulainen. 2004. Structure and dynamics of sphingomyelin bilayer: insight gained through systematic comparison to phosphatidylcholine. *Biophys. J.* 87:2976–2989.

21. Térová, B., R. Heczko, and J. P. Slotte. 2005. On the importance of the phosphocholine methyl groups for sphingomyelin/cholesterol interactions in membranes: a study with ceramide phosphoethanolamine. *Biophys. J.* 88:2661–2669.

22. Boggs, J. M. 1987. Lipid intermolecular hydrogen bonding: influence on structural organization and membrane function. *Biochim. Biophys. Acta.* 906:353–404.

23. Ho, C., and C. D. Stubbs. 1992. Hydration at the membrane protein-lipid interface. *Biophys. J.* 63:897–902.

24. Parasassi, T., M. Di Stefano, M. Loiero, G. Ravagnan, and E. Gratton. 1994. Cholesterol modifies water concentration and dynamics in phospholipid bilayers: a fluorescence study using Laurdan probe. *Biophys. J.* 66:763–768.

25. Klymchenko, A. S., G. Duportail, A. P. Demchenko, and Y. Mély. 2004. Bimodal distribution and fluorescence response of environment-sensitive probes in lipid bilayers. *Biophys. J.* 86:2929–2941.

26. Chou, P.-T., M. L. Martinez, and J.-H. Clements. 1993. Reversal of excitation behavior of proton-transfer vs. charge-transfer by dielectric perturbation of electronic manifolds. *J. Phys. Chem.* 97:2618–2622.

27. Swinney, T. C., and D. F. Kelley. 1993. Proton transfer dynamics in substituted 3-hydroxyflavones: Solvent polarization effects. *J. Chem. Phys.* 99:211–221.

28. Ormson, S. M., R. G. Brown, F. Vollmer, and W. Rettig. 1994. Switching between charge- and proton-transfer emission in the excited state of a substituted 3-hydroxyflavone. *J. Photochem. Photobiol. A. Chem.* 81:65–72.

29. Klymchenko, A. S., and A. P. Demchenko. 2003. Multiparametric probing of intermolecular interactions with fluorescent dye exhibiting excited state intramolecular proton transfer. *Phys. Chem. Chem. Phys.* 5:461–468.

30. Duportail, G., A. Klymchenko, Y. Mély, and A. Demchenko. 2001. Neutral fluorescence probe with strong ratiometric response to surface charge of phospholipid membranes. *FEBS Lett.* 508:196–200.

31. Klymchenko, A. S., V. G. Pivovarenko, and A. P. Demchenko. 2003. Elimination of hydrogen bonding effect on solvatochromism of 3-hydroxyflavones. *J. Phys. Chem. A.* 107:4211–4216.

32. Shynkar, V. V., A. S. Klymchenko, E. Piémont, A. P. Demchenko, and Y. Mély. 2004. Dynamics of intermolecular hydrogen bonds in the excited states of 4′-dialkylamino-3-hydroxyflavones. On the pathway to ideal fluorescent hydrogen bonding sensor. *J. Phys. Chem. A.* 108:8151–8159.

33. Klymchenko, A. S., Y. Mély, A. P. Demchenko, and G. Duportail. 2004. Simultaneous probing of hydration and polarity of lipid bilayers with 3-hydroxyflavone fluorescent dyes. *Biochim. Biophys. Acta.* 1665:6–19.

34. Klymchenko, A. S., G. Duportail, T. Oztürk, V. G. Pivovarenko, Y. Mély, and A. P. Demchenko. 2002. Novel two-band ratiometric fluorescence probes with different location and orientation in phospholipid membranes. *Chem. Biol.* 9:1199–1208.

35. Wiener, M. C., and S. H. White. 1992. Structure of a fluid dioleoylphosphatidylcholine bilayer determined by joint refinement of x-ray and neutron diffraction data. III. Complete structure. *Biophys. J.* 61: 437–447.

36. Hope, M. J., M. B. Bally, G. Webb, and P. R. Cullis. 1985. Production of large unilamellar vesicles by a rapid extrusion procedure. Characterization of size distribution, trapped volume and ability to maintain a membrane potential. *Biochim. Biophys. Acta.* 812:55–65.

37. Shynkar, V. V., A. S. Klymchenko, Y. Mély, G. Duportail, and V. G. Pivovarenko. 2004. Anion formation of 4′-(dimethylamino)-3-hydroxyflavone in phosphatidylglycerol vesicles induced by HEPES buffer: a steady-state and time-resolved fluorescence investigation. *J. Phys. Chem. B.* 108:18750–18755.

38. Siano, D. B., and D. E. Metzler. 1969. Band shapes of the electronic spectra of complex molecules. *J. Chem. Phys.* 51:1856–1861.

39. de Almeida, R. F. M., A. Fedorov, and M. Prieto. 2003. Sphingomyelin/ phosphatidylcholine/cholesterol phase diagram: Boundaries and composition of lipid rafts. *Biophys. J.* 85:2406–2416.

40. Prendergast, F. G., R. P. Haugland, and P. J. Callahan. 1981. 1-[4-(Trimethylamino)phenyl]-6-phenylhexa-1,3,5-triene: synthesis, fluorescence properties and use as a probe of lipid bilayers. *Biochemistry.* 20:7333–7338.

41. Vincent, M., and J. Gallay. 1983. Steroid-lipid interactions in sonicated DPPC vesicles: a steady-state and time-resolved fluorescence anisotropy study with all trans-1,6-diphenyl-1,3,5-hexatriene as probe. *Biochem. Biophys. Res. Commun.* 113:799–810.

42. Genz, A., J. F. Holzwarth, and T. Y. Tsong. 1986. The influence of cholesterol on the main phase transition of unilamellar dipalmitoylphosphatidylcholine vesicles. *Biophys. J.* 50:1043–1051.

43. Cevc, G., and D. Marsh. 1987. Phospholipid Bilayers. Physical Principles and Models. John Wiley & Sons, New York.

44. McIntosh, T. J. 1978. The effect of cholesterol on the structure of phosphatidylcholine bilayers. *Biochim. Biophys. Acta.* 513:43–58.

45. Kaiser, R. D., and E. London. 1998. Location of diphenylhexatriene (DPH) and its derivatives within membranes: comparison of different fluorescence quenching analyses of membrane depth. *Biochemistry.* 37:8180–8190.

46. Radhakrishnan, A., and H. M. McConnell. 1999. Condensed complexes of cholesterol and phospholipids. *Biophys. J.* 77:1507–1517.

47. Hung, W. C., M. T. Lee, F. Y. Chen, and H. W. Huang. 2007. The condensing effect of cholesterol in lipid bilayers. *Biophys. J.* 92:3960–3967.

48. Kupiainen, M., E. Falck, S. Ollila, P. Niemelä, A. A. Gurtovenko, M. T. Hyvönen, M. Patra, M. Karttunen, and I. Vattulainen. 2005. Free volume properties of Sphingomyelin, DMPC, DPPC and PLPC bilayers. *J. Comput. Theor. Nanosci.* 2:401–413.

49. Falck, E., M. Patra, M. Karttunen, M. T. Hyvönen, and I. Vattulainen. 2004. Impact of cholesterol on voids in phospholipid membranes. *J. Chem. Phys.* 121:12676–12689.